Published in final edited form as:
Genesis. 2013 August ; 51(8): 587–595. doi:10.1002/dvg.22401.

Functional defect of peripheral neutrophils in mice with induced deletion of CXCR2

LiPing Liu[§], **MeiZhang Li**[§,#], **Lisa C. Spangler**, **Charles Spear**, **Mike Veenstra**, **Lindsey Darnall**, **Cathleen Chang**, **Anne C. Cotleur**, and **Richard M. Ransohoff**[*]
Neuroinflammation Research Centre, Department of Neuroscience, Lerner Research Institute, Cleveland Clinic, 9500 Euclid Avenue, Cleveland, Ohio, USA 44195

Abstract

Type 2 CXC chemokine receptor CXCR2 plays roles in development, tumorigenesis and inflammation. CXCR2 also promotes demyelination and decreases remyelination by actions toward hematopoietic cells and non-hematopoietic cells. Germline CXCR2 deficient (*Cxcr2*$^{-/-}$) mice reported in 1994 revealed the complexity of CXCR2 function and its differential expression in varied cell-types. Here, we describe *Cxcr2*$^{fl/fl}$ mice for which the targeting construct was generated by recombineering based on homologous recombination in *E. coli.* Without recombination *Cxcr2*$^{fl/fl}$ mice have CXCR2 expression on neutrophils in peripheral blood, bone marrow and spleen. *Cxcr2*$^{fl/fl}$ mice were crossed to *Mx-Cre* mice in which Cre recombinase is induced by type I interferons, elicited by injection with polyinosinic-polycytidylic acid (poly(I:C)). CXCR2-deficient neutrophils were observed in poly(I:C) treated *Cxcr2*$^{fl/fl}$*::Mx-Cre*$^{+}$ (*Cxcr2*-CKO) mice, but not in poly(I:C) treated *Cxcr2*$^{fl/+}$*::Mx-Cre*$^{+}$ mice. CXCR2 deletion was mainly observed peripherally but not in the CNS. *Cxcr2*-CKO mice showed impaired neutrophil migration in sterile peritonitis. *Cxcr2*-CKO mice reported here will provide a genetic reagent to dissect roles of CXCR2 in the neutrophil granulocyte lineage. Furthermore *Cxcr2*$^{fl/fl}$ mice will provide useful genetic models to evaluate CXCR2 function in varied cell populations.

Keywords

CXCR2; chemokine; chemokine receptor; conditional KO mice; neutrophil

Introduction

CXCR2 was cloned in 1991(Holmes et al. 1991; Murphy & Tiffany 1991) and is expressed on myeloid cells in the periphery as well as on oligodendrocyte progenitor cells (OPCs) in the central nervous system (CNS). With its seven differentially-regulated ligands, CXCR2 shows multiple additional functions beyond chemoattraction for myeloid cell trafficking (Cacalano et al. 1994). On OPCs in the developing rodent spinal cord, CXCR2 interacts with CXCL1, arresting migrating OPCs during development, and promoting the OPC proliferative response to PDGFA (Tsai et al. 2002). CXCR2 also plays a role in wound healing (Devalaraja et al. 2000), acetaminophen hepatotoxicity (Hu & Colletti 2010), bone mineralization, intramembranous bone formation (Bischoff et al. 2011), spontaneous tumorigenesis (Jamieson et al. 2012), cancer metastasis and chemoresistance (Acharyya et

[*]Correspondence: ransohr@ccf.org, Tel: 216-444-0627, Fax: 216-445-7927.
[#]Current address: Laboratory of Biochemistry and Molecular Biology, School of Life Sciences, Yunnan University, Kunming 650091, P. R. China.
[§]These authors contributed equally to this work.

There is no conflict of interest to declare.

al. 2012). Recently we and others found that CXCR2 function on neutrophils plays a role in both autoimmune and toxic demyelination (Liu et al. 2010a; Carlson et al. 2008) as well as myelin repair (Liu et al. 2010b). Importantly, CXCR2 plays orthologous roles in humans and rodents (Mihara et al. 2005).

CXCR2 deficient mice (*Cxcr*2$^{-/-}$) (Cacalano et al. 1994) are fragile and infertile, which complicates breeding and disease modeling. We generated *Cxcr2*$^{fl/fl}$ mice to extend research into cell-type specific and inducible deletion of this pleiotropic receptor. In transgenic mice expressing inducible Cre recombinase under control of the *Mx1* promoter (*Mx-Cre*), our induction protocol efficiently deleted the floxed *Cxcr*2 gene in hematopoietic cells. *Cxcr*2-CKO mice 4 wks after poly(I:C) injections showed deletion of CXCR2 on peripheral neutrophils and deficient neutrophil migration. Our data indicate that *Cxcr2*$^{fl/fl}$ mice provide a useful reagent to advance current research into CXCR2 and its chemokine ligands in inflammation, cancer and neurological disease.

Results and Discussion

Generation of Cxcr2 conditional knockout (*Cxcr*2-CKO) mice

A *Cxcr*2 conditional targeting construct was generated by recombineering and electroporated into C57BL/6 ES cells, which were screened by Southern blotting (Fig. 1a). Twenty-five candidate ES cell lines were verified both through 3′ screening (Fig. 1a, data not shown) and sequence analysis through the loxP and FRT sites (data not shown). One correct ES clone (clone 1) from seven candidates was re-confirmed by sequence analysis of the loxP and FRT sites (data not shown).

Chimeric founder mice harboring the *Cxcr2*$^{fl/+}$ allele were intercrossed to generate *Cxcr2*$^{fl/fl}$ mice. To create the *Cxcr*2-CKO mouse line, *Cxcr2*$^{fl/fl}$ mice were bred to *Mx*-Cre mice (Kuhn et al., 1995) and intercrossed to generate *Cxcr2*$^{fl/+}$*::Mx-Cre*$^{+}$ and *Cxcr2*$^{fl/fl}$*::Mx-Cre*$^{+}$ genotypes.

Expression of CXCR2 in *Cxcr2*$^{fl/fl}$ mice

The *Cxcr2*^{fl} allele was detected with F5FRT and R6FRT primers (Figure 1b-A). CXCR2 was detected by flow cytometry on Ly6G+ neutrophils of *Cxcr2*$^{fl/fl}$ mice, at similar frequency and mean fluorescence intensity to *Cxcr*2$^{+/+}$ mice (Figure 2). Spleen and bone marrow from *Cxcr2*$^{fl/fl}$ and *Cxcr2*$^{+/+}$ mice showed similar CXCR2 expression patterns as peripheral blood (Supplementary 2, data not shown).

CXCR2 is stably deleted by poly(I:C) in *Mx-Cre::Cxcr*2 CKO mice

Intraperitoneal poly(I:C) injections induced Cre recombinase in *Cxcr2*$^{fl/fl}$*::Mx-Cre*$^{+}$ and *Cxcr2*$^{fl/+}$*::Mx-Cre*$^{+}$ mice. Analysis of genomic DNA after poly(I:C) injection showed the *Cxcr2* deletion product in samples from *Cxcr2*$^{fl/fl}$*::Mx-Cre*$^{+}$ and *Cxcr2*$^{fl/+}$*::Mx-Cre*$^{+}$ but not *Cxcr2*$^{+/+}$*::Mx-Cre*$^{+}$ or *Cxcr2*$^{fl/fl}$ mice (Figure 1b).

We analyzed CXCR2 protein product on blood leukocytes weekly after poly(I:C) induction. In *Cxcr2*-CKO mice, CXCR2 deletion on blood neutrophils was time-dependent. To our surprise, deletion of CXCR2 was first observed at 3wks post injection (pi) (Figure 3B). At 4 wks pi, most *Cxcr2*-CKO mice showed >90% of blood neutrophils were CXCR2-negative (calculated by the ratio of CXCR2 negative cells in total Ly6G+ cells) (Figure 3B, supplementary 2). Cells from the spleen and bone marrow showed equivalent CXCR2 deletion in the neutrophil lineage (Supplementary 2). Monitoring until 18 wks pi, showed stable deletion of CXCR2 (Figure 3B). *Cxcr2*-CKO mice showed considerable delay in the appearance of CXCR2-negative circulating neutrophils, as compared to previous studies

targeting other cell surface molecules where target-deficient cells are detected within a few days (Tiedt et al. 2008; Ulyanova et al. 2007; Yan, 2008). Before appearance of CXCR2-deficient leukocytes in the circulation, necessary events include activating the Mx1 promoter with poly(I:C)-induced type I IFN, producing Cre recombinase, and recombining the floxed gene. Thereafter, turn-over of the targeted protein or cells expressing that protein must occur before target-negative cells predominate (Nagy, 2000). It remains plausible that retention of CXCR2-deficient neutrophil progenitors in bone marrow (Köhler et al. 2011) accounts for the failure of CXCR2-negative neutrophils to accumulate in the bloodstream. In particular, neutrophil progenitors remaining CXCR2+ will be privileged for bone marrow exit and that population must be exhausted before CXCR2-deficient cells will appear in the periphery. *Cxcr2*$^{fl/fl}$*::Mx-Cre*$^{+}$ mice were born at expected Mendelian ratios and showed normal weight, behavior, fertility and life span. *Cxcr*2-CKO mice lost weight compared to littermates after efficient CXCR2 deletion on neutrophils (data not shown), reminiscent of the failure-to-thrive phenotype in germline *Cxcr*2$^{-/-}$ mice.

CXCR2-deficient neutrophils show defective ligand scavenging

Signaling chemokine receptors such as CXCR2 scavenge their ligands (Cardona et al. 2008). CXCR2 ligand CXCL1 was undetectable in plasma of *Cxcr2*$^{fl/fl}$ or *Cxcr2*$^{+/+}$ mice, while being present at high levels in plasma from positive control *Cxcr2*$^{-/-}$ animals showing that the *Cxcr2*$^{fl/fl}$ targeted allele scavenged efficiently (Figure 4, data not shown). *Cxcr2*-CKO mice with more than 90% CXCR2 deletion on neutrophils showed dramatically increased plasma CXCL1 in the serum comparable to those in *Cxcr2*$^{-/-}$ mice (Figure 4). However, *Cxcr2*-CKO mice with less than 90% CXCR2 deletion on neutrophils showed comparable levels of plasma CXCL1 to control mice (Figure 4). These results indicate that near-complete induction of CXCR2 deficiency on peripheral neutrophils is required to abrogate the scavenging of CXCL1.

Dose-dependent recombination induced by poly(I:C) in periphery but not CNS of *Cxcr2*-CKO mice

After 4 injections at 2.5mg/kg poly(I:C), we observed 30% deletion of CXCR2 on neutrophils while 15mg/kg poly(I:C) induced >90% deletion on neutrophils at 4 wks pi, 6 wks pi and 8 wks pi (Figure 5A). Concerned with effects of the 15mg/kg poly(I:C), including inflammatory cytokine (TNF-α, IL-6, or IFNγ) production and sickness behavior (Cunningham et al. 2007) which could confound data analysis for neuroinflammatory disease models, we examined the timing of poly(I:C) injections at lower doses of poly(I:C). At 5mg/kg poly(I:C) with assay 4 wks pi, we observed partial CXCR2 deletion from circulating neutrophils of mice injected at ages >8wks. Using the same dose and timing of assay, we observed >90% CXCR2 deletion on neutrophils of most mice injected at 4wks of age (Figure 5B). Compared to 5 mg/kg, high-doses (15 mg/kg) of poly(I:C) once every other day for 4 injections did not alter the extent or kinetics for generating CXCR2-negative blood neutrophils in young mice (~3–4 wks old). However, high-dose poly(I:C) caused more-efficient CXCR2 deletion on neutrophils in older mice (>8 wks old). We concluded that, 5 mg/kg was an appropriate dose of poly(I:C) for the CXCR2 deletion in young *Cxcr2*-CKO mice avoiding the neurotoxic effects caused by high-dose poly(I:C).

To determine whether the deletion of CXCR2 differed in the periphery from the CNS, we performed qPCR to examine Cre expression. Cre recombinase induction in spleen (200-fold) was far greater than that in the brain (six-fold) (Figure 5C). To determine if low-level induction of Cre recombinase mediated recombination in CNS parenchyma, we crossed *Mx-Cre* mice to reporter ROSA26mTmG mice (Muzumdar et al. 2007), and monitored recombination as conversion from tomato red to GFP labeled cells in the CNS. There were no green neuroepithelial parenchymal CD45 negative cells in the CNS 4wks after injection

of 5 mg/kg poly(I:C) by flow cytometry (data not shown), which is consistent with a previous finding (Kuhn et al., 1995).

Decreased migration of CXCR2-deficient neutrophils in sterile peritonitis

To assess neutrophil migration toward an inflammatory stimulus in *Cxcr2*-CKO mice, the sterile irritant thioglycollate was administered i.p.. Total peritoneal cell number was reduced by about 50% in *Cxcr2*-CKO mice ($0.32\pm0.02\times10^6$/mL) as compared with the $Cxcr2^{fl/+}$::*Mx-Cre*$^+$ group ($0.59\pm0.10\times10^6$/mL, P=0.022) due to the virtual absence of recruited neutrophils in *Cxcr2*-CKO mice (Figure 6A and B). Giemsa-stained cytospin preparations from the peritoneal cavity showed more macrophage-like cells in *Cxcr2*-CKO mice than in $Cxcr2^{fl/+}$::*Mx-Cre*$^+$ mice (Figure 6C). In $Cxcr2^{fl/+}$::*Mx-Cre*$^+$ mice, CXCR2 expression was downregulated on infiltrated peritoneal neutrophils (Figure 6D) suggesting receptor engagement during migration.

Our current data indicate that the floxed *Cxcr*2 gene was deleted by induction of Cre recombinase in $Cxcr2^{fl/fl}$ mice, providing opportunities to elucidate the functions of CXCR2 and its many chemokine ligands in murine models of human disorders such as neurodegenerative disease and cancer.

Methods

Mice

The *Cxcr*2 targeting construct for generation of a conditional *Cxcr*2 allele was built by recombineering (Liu et al. 2003), based on homologous recombination in *E. coli* and applied to modifying BACs. The *Cxcr*2 targeting construct DNA was electroporated into C57BL/6 ES cells. Twenty-five positive candidates from the total 192 ES clones were screened and verified by both Southern hybridization and genomic DNA sequencing. One targeted ES clone was injected into 129/SvEv blastocysts to create chimeric mice. Chimeric founder mice (C57BL/6×129/SvEv) were backcrossed with C57BL/6 mice. Germline transmission of the C*xcr*2^{flox} (C*xcr*2^{fl}) allele was confirmed by Southern hybridization and PCR genotyping. To establish the *Cxcr*2-CKO mouse line, *Cxcr*2$^{fl/fl}$ mice were further bred to *Mx-Cre* mice (Stock Number: 003556; Strain name: B6.Cg-Tg (*Mx1-Cre*)1Cgn/J from the Jackson Laboratory). Conditional knockout mice include the *Cxcr*2-CKO mice. Control mice used for conditional deletion studies included $Cxcr2^{fl/+}$::*Mx-Cre*$^+$ or *Cxcr*2$^{fl/fl}$ genotypes. ROSA26mTmG mice were obtained from The Jackson Laboratory. All mouse studies were approved by the Institutional Animal Care and Use Committee (IACUC) at the Cleveland Clinic (Cleveland, OH).

Genotyping

The *Cxcr*2^{fl} allele was detected with primers which consist of forward primer F5FRT (AGGGAATAGGGGATATTTGG) and reverse primer R6FRT (GCTTGGCTGGACGTAAACTC). Mice were genotyped by amplification of genomic DNA obtained by tail biopsy as shown by figure 1b. The *Cxcr*2$^+$ allele was detected with primers which consist of forward primer F5FRT (AGGGAATAGGGGATATTTGG) and reverse primer R3LoxP2 (CGTCTGTGCCTTCTAAGCCT). This PCR reaction yields a 450bp fragment from the *Cxcr*2^{fl} allele and 640bp fragment from the *Cxcr*2$^+$ allele. The presence of the deleted allele was detected with LoxPF3 primer (CTACTAGCATGTTTGAGCCC) and FrtR primer (CTTGAATGAGGATGGTTGTT), the amplified fragment measured 400bp (figure 1b). This band was purified with a QIAGEN PCR Purification Kit (Invitrogen) according to the kit manual and the purified product was sequenced by the Molecular Core Facility in the Cleveland Clinic. For *Mx-Cre* detection, we redesigned specific primers. One primer is located on the Mx1 promoter (Hug et al. 1988)

and another one is on the *Cre* gene. The PCR product from this pair of primers detects *Cre* genes expressed under the Mx1 promoter (forward primer: MxPF1: TCCCAACCTCAGTACCAAGC, and reverse primer: Cre2: ATTCTCCCACCGTCAGTACG, the DNA product measures 800bp (Supplementary data 1). GAPDH primers were used for positive controls as described before (Liu et al. 2010a).

Injection of poly(I:C) and analysis of CXCR2 deletion

4 or 8 wks old mice were treated with different doses of poly(I:C) (P1530, Sigma, St. Louis, MO) (2.5 mg/kg, 5 mg/kg, 15 mg/kg) as indicated once every other day for a total of 4 injections. The time after poly(I:C) injection was counted from the last day of injection (day 0) as days post injection (pi.).

Deletion of CXCR2 from freshly isolated peripheral leukocytes was determined by flow cytometry. Blood was drawn before the first poly(I:C) injection (time point 0) and once per week for the indicated time. Red blood cells were lysed with red blood cell lysis buffer as decribed previously (Liu et al. 2010a). For the analysis of percentage of deleted CXCR2 on neutrophils, the peripheral leukocytes were stained with antibody mixtures of CD45APC (Clone: 30-F11; Biolegend), CXCR2PE (Clone: 242216; R&D) and Ly6GFITC (Clone: 1A8; Biolegend) and analyzed with flow cytometry as described previously (Liu et al. 2010a). The percentage of CXCR2 deleted neutrophils was determined as the ratio of CXCR2 negative neutrophils to the total $Ly6G^+$ neutrophil population. The percentage of neutrophils in a total blood sample was determined as the ratio of $Ly6G^+$ in total $CD45^+$ cells. Analysis was performed with an LSRII (BD Biosciences) equipped with CellQuest software (BD Biosciences), and 10,000 events per sample, were acquired. Data were analyzed with FlowJo software (Tree Star).

ELISA

At the indicated time-points, blood samples were obtained by submandibular puncture. The level of CXCL1 was detected in the sera by ELISA (Duoset, R&D Systems), as described by the manufacturer.

TG-induced peritonitis

To study the migration of neutrophils to the site of inflammation in the periphery, inflammation in the peritoneal cavity was induced by using 4% TG medium (Sigma-Aldrich, USA) in ddH_2O. Autoclaved TG solution was aged in the dark at 4°C for at least one week. Mice were injected i.p. with 4% TG solution (1 mL/20 g mouse). After 2 hours, mice were sacrificed, and peritoneal leukocytes and blood samples were collected. The neutrophil content in the peritoneal cavity and the blood was determined by flow cytometry. Total cell counts from the peritoneum were performed by hemocytometer (Hausser Scientific, Horsham, PA, USA) immediately following peritoneal cell collection. Cells were stained with antibodies as indicated in data and analyzed by flow cytometry. Some of the cells from the peritoneum were cytospun for Wright-Giemsa staining according to the manufacturer's protocol.

Statistical analysis

Data are expressed as mean ± SD. Multiple comparisons were statistically evaluated by 1-way ANOVA using Prism 4 (GraphPad Software). The Students-*t*-test was used for the comparisons of cytokine content, the percentage of CXCR2 deletion. A p value <0.05 was considered as significant. *P<0.05, **P<0.01.

Supplementary Material

Refer to Web version on PubMed Central for supplementary material.

Acknowledgments

This work was supported by National Institutes of Health Grants R01NS032151 (R.M.R) and NS051400 (R.M.R).

We thank the Murine Molecular Constructs Laboratory from the Mouse Biology Program at UC Davis and the Case Transgenic and Targeting Facility at Case Western Reserve University. We thank Dr. Qi Shi (Neuroscience Department, Cleveland Clinic) for help with genotyping the mice; we thank the LRI-Flow Core for providing excellent service. Thank you also to Dr. Christine L. White (Molecular Genetics Department) for providing primers and techniques for checking the activation of interferons. ML is supported by funding from Yunnan Province High-tech Talent Introduction Project and the National Natural Science Foundation of China No.30960091 and No. 81271330.

References

Acharyya S, Oskarsson T, Vanharanta S, Malladi S, Kim J, Morris PG, Manova-Todorova K, Leversha M, Hogg N, Seshan VE, Norton L, Brogi E, Massagué J. A CXCL1 paracrine network links cancer chemoresistance and metastasis. Cell. 2012; 150:165–171. [PubMed: 22770218]

Bischoff DS, Sakamoto T, Ishida K, Makhijani NS, Gruber HE, Yamaguchi DT. CXC receptor knockout mice: characterization of skeletal features and membranous bone healing in the adult mouse. Bone. 2011; 48:267–274. [PubMed: 20870046]

Cacalano G, Lee J, Kikly K, Ryan AM, Pitts-Meek S, Hultgren B, Wood WI, Moore MW. Neutrophil and B cell expansion in mice that lack the murine IL-8 receptor homolog. Science. 1994; 265:682–684. [PubMed: 8036519]

Cardona AE, Li M, Liu L, Savarin C, Ransohoff RM. Chemokines in and out of the central nervous system: much more than chemotaxis and inflammation. J Leukoc Biol. 2008; 84:587–594. [PubMed: 18467654]

Carlson T, Kroenke M, Rao P, Lane TE, Segal B. The Th17-ELR+ CXC chemokine pathway is essential for the development of central nervous system autoimmune disease. J Exp Med. 2008; 205:811–823. [PubMed: 18347102]

Cunningham C, Campion S, Teeling J, Felton L, Perry VH. The sickness behaviour and CNS inflammatory mediator profile induced by systemic challenge of mice with synthetic double-stranded RNA (poly I:C). Brain Behav Immun. 1997; 21:490–502. [PubMed: 17321719]

Devalaraja RM, Nanney LB, Du J, Qian Q, Yu Y, Devalaraja MN, Richmond A. Delayed wound healing in CXCR2 knockout mice. J Invest Dermatol. 2000; 115:234–244. [PubMed: 10951241]

Holmes WE, Lee J, Kuang WJ, Rice GC, Wood WI. Structure and functional expression of a human interleukin-8 receptor. Science. 1991; 253:1278–1280. [PubMed: 1840701]

Hu B, Colletti LM. CXC receptor-2 knockout genotype increases X-linked inhibitor of apoptosis protein and protects mice from acetaminophen hepatotoxicity. Hepatology. 2010; 52:691–702. [PubMed: 20683965]

Hug H, Costas M, Staeheli P, Aebi M, Weissmann C. Organization of the murine Mx gene and characterization of its interferon- and virus-inducible promoter. Mol Cell Biol. 1988; 8:3065–3079. [PubMed: 2974922]

Jamieson T, Clarke M, Steele CW, Samuel MS, Neumann J, Jung A, Huels D, Olson MF, Das S, Nibbs RJ, Sansom OJ. Inhibition of CXCR2 profoundly suppresses inflammation-driven and spontaneous tumorigenesis. J Clin Invest. 2012; 122:3127–3144. [PubMed: 22922255]

Köhler A, De Filippo K, Hasenberg M, van den Brandt C, Nye E, Hosking MP, Lane TE, Männ L, Ransohoff RM, Hauser AE, Winter O, Schraven B, Geiger H, Hogg N, Gunzer M. G-CSF-mediated thrombopoietin release triggers neutrophil motility and mobilization from bone marrow via induction of Cxcr2 ligands. Blood. 2011; 117:4349–57. [PubMed: 21224471]

Kuhn R, Schwenk F, Aguet M, Rajewsky K. Inducible gene targeting in mice. Science. 1995; 269:1427–1429. [PubMed: 7660125]

Liu L, Belkaldi A, Darnall L, Hu T, Drescher C, Cotleur AC, Padovani-Claudio D, He T, Choi K, Lane TE, Miller RH, Ransohoff RM. CXCR2-positive neutrophils are essential for cuprizone-induced demyelination: relevance to multiple sclerosis. Nat Neurosci. 2010a; 13:319–326. [PubMed: 20154684]

Liu L, Darnall L, Hu T, Choi K, Lane TE, Ransohoff RM. Myelin repair is accelerated by inactivating CXCR2 on nonhematopoietic cells. J Neurosci. 2010b; 30:9074–9083. [PubMed: 20610741]

Liu P, Jenkins NA, Copeland NG. A highly efficient recombineering-based method for generating conditional knockout mutations. Genome Res. 2003; 13:476–484. [PubMed: 12618378]

Mihara K, Smit MJ, Krajnc-Franken M, Gossen J, Rooseboom M, Dokter W. Human CXCR2 (hCXCR2) takes over functionalities of its murine homolog in hCXCR2 knockin mice. Eur J Immunol. 2005; 35:2573–2582. [PubMed: 16094689]

Murphy PM, Tiffany HL. Cloning of complementary DNA encoding a functional human interleukin-8 receptor. Science. 1991; 253:1280–1283. [PubMed: 1891716]

Muzumdar MD, Tasic B, Miyamichi K, Li L, Luo L. A global double-fluorescent Cre reporter mouse. Genesis. 2007; 45:593–605. [PubMed: 17868096]

Nagy A. Cre recombinase: the universal reagent for genome tailoring. Genesis. 2000; 26:116–117. [PubMed: 10686602]

Tiedt R, Hao-Shen H, Sobas MA, Looser R, Dirnhofer S, Schwaller J, Skoda RC. Ratio of mutant JAK2-V617F to wild-type Jak2 determines the MPD phenotypes in transgenic mice. Blood. 2008; 111:3931–3940. [PubMed: 18160670]

Tsai HH, Frost E, To V, Robinson S, ffrench-Constant C, Geertman R, Ransohoff RM, Miller RH. The chemokine receptor CXCR2 controls positioning of oligodendrocyte precursors in developing spinal cord by arresting their migration. Cell. 2002; 110:373–383. [PubMed: 12176324]

Ulyanova T, Priestley GV, Nakamoto B, Jiang Y, Papayannopoulou T. VCAM-1 ablation in nonhematopoietic cells in MxCre+ VCAM-1f/f mice is variable and dictates their phenotype. Exp Hematol. 2007; 35:565–571. [PubMed: 17379066]

Yan J, Chen S, Zhang Y, Li X, Li Y, Wu X, Yuan J, Robling AG, Kapur R, Chan RJ, Yang FC. Rac1 mediates the osteoclast gains-in-function induced by haploinsufficiency of Nf1. Hum Mol Genet. 2008; 17:936–948. [PubMed: 18089636]

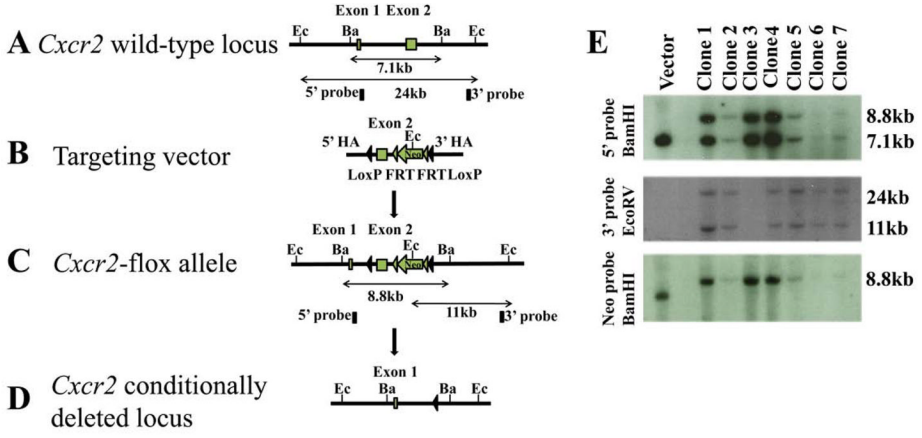

Figure 1. Generation of a conditional *Cxcr*2 allele and genotype determination of conditional knockouts by PCR

a. The strategy for *Cxcr2*^{fl} mouse generation. (A). Schematic diagram of the *Cxcr*2 wild-type genomic locus demonstrating a classic two-exon gene structure that is indicated by two blank boxes. In order to screen for the targeted *Cxcr*2^{fl} mutant allele, both 5′ and 3′ Southern blot probes (filled boxes) were designed in the genomic regions inside of two homologous arms (HA). Restriction enzymes are in the abbreviated form: Ec, EcoRV and Ba, BamHI. (B). A *Cxcr*2^{fl} targeting vector was constructed by recombineering. The targeting region includes a 2-kb 5′ HA, a LoxP site that flanks *Cxcr*2 exon2, a *Frt-PGKNeo-Frt* cassette that is downstream of *Cxcr*2 exon2 flanked by another LoxP site and a 3-kb 3′ HA. (C). Schematic demonstration of the targeted *Cxcr*2^{fl} allele. In Southern blot screening, an 8.8kb-BamHI targeted band (5′ probe) and an 11kb-EcoRV targeted band (3′ probe) are expected. (D). Schematic diagram depicting the conditional deletion of the *Cxcr*2 gene through Cre-mediated recombination. (E). Seven targeted embryonic stem cells were screened by Southern blot. 7.1kb wild-type and 8.8kb targeted BamHI bands were detected by the 5′ Southern probe. 24kb wild-type and 11kb mutant-type EcoRV bands are detected by the 3′ Southern probe. An 8.8kb targeted BamHI band is detected by using the PGK-neo probe. Targeting vector was used as the control. **b. Genotype determination of *Cxcr2*-CKO mice by PCR.** (A) Strategy for designing PCR primers to detect the Wt locus, the flox allele and the deletion of the flox allele. The primers are shown as arrows. (B) PCR amplification of the genomic DNA using primers for the flox gene before injection of poly(I:C); the higher band (~650 bp) indicates the wild-type allele and the lower band (~450 bp) indicates the flox allele (top). PCR amplification of the genomic DNA using primers to detect the deletion of the flox allele (~400 bp) after poly(I:C) induced recombination (bottom). (C) PCR amplification of the genomic DNA using primers to detect the *Mx-Cre* transgenes (top). The details for designing the primers specific for *Mx-Cre* are described in supplementary data 1. The bottom figure shows representive PCR results of GAPDH for quality control of the genomic DNA used for (B) and (C).

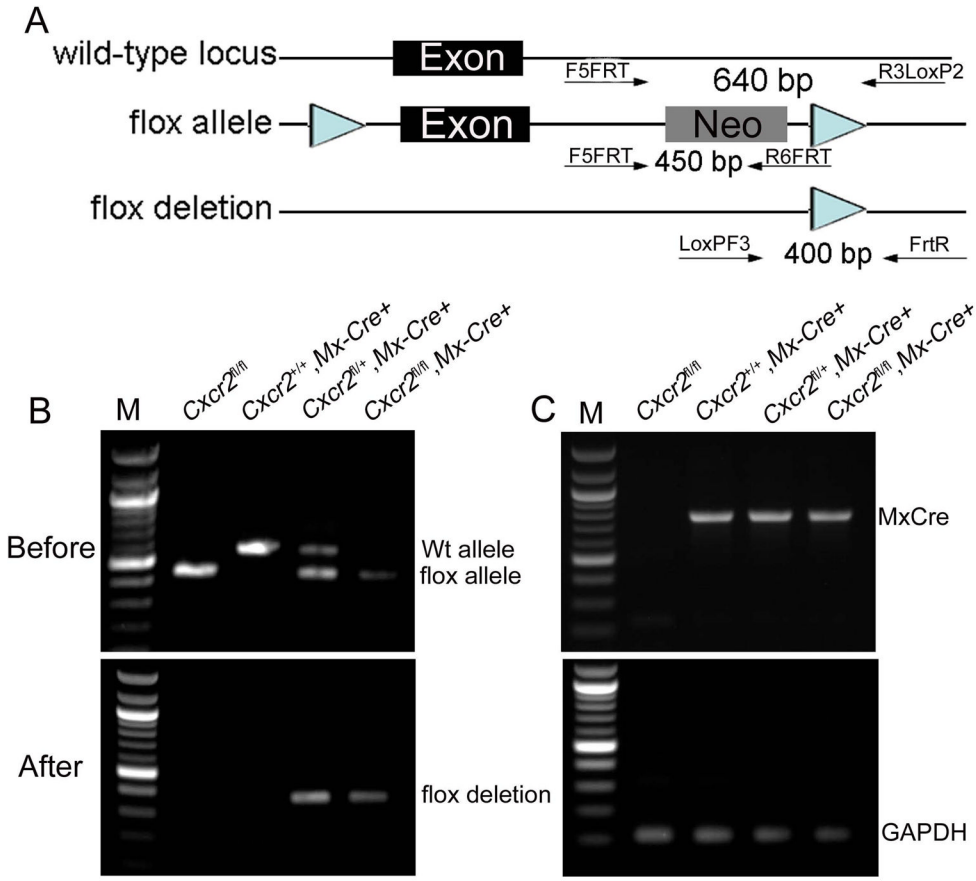

Figure 2. Expression of CXCR2 in *Cxcr2*$^{fl/fl}$ mice

Peripheral blood cells from *Cxcr*2$^{fl/+}$ and *Cxcr*2$^{fl/fl}$ mice (bottom) stained with Ly6G and CXCR2 antibodies were analyzed by flow cytometry. Cells from *Cxcr*2$^{+/+}$ and *Cxcr*2$^{-/-}$ mice (top) were used as positive and negative controls respectively. These data represent at least three independent experiments.

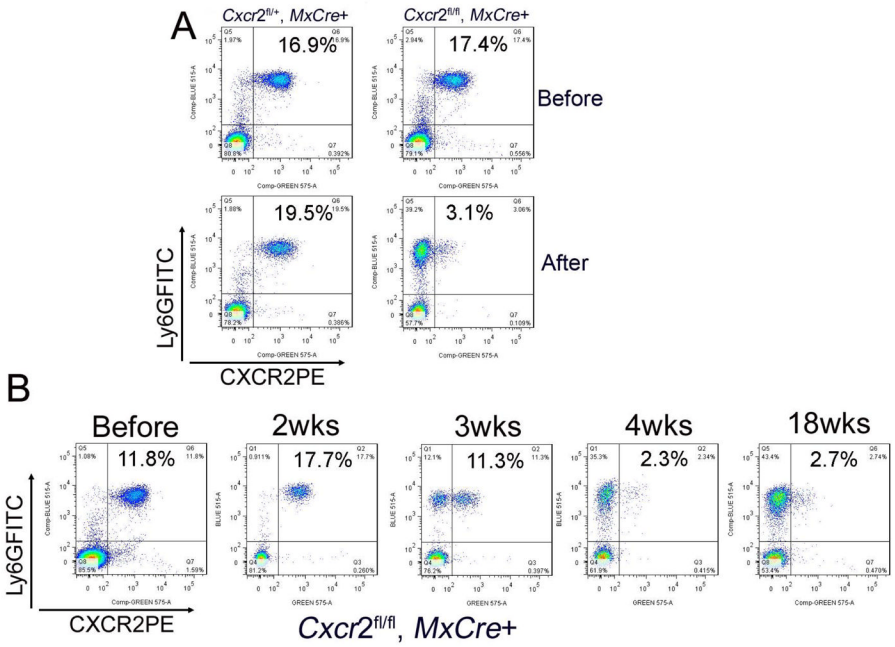

Figure 3. CXCR2 is stably deleted by poly(I:C) in *Mx-Cre::Cxcr2* CKO mice

(A) Efficient deletion of CXCR2 after poly(I:C) injection. Peripheral blood cells from *Cxcr2*$^{fl/+}$*::Mx-Cre*$^{+}$ and *Cxcr2*$^{fl/fl}$*::Mx-Cre*$^{+}$ mice before injection (figure 3A, top) and 4 wks after injection (figure 3A, bottom), were stained with Ly6GFITC and CXCR2PE antibodies and were analyzed by flow cytometry. These data represent at least three independent experiments. (B) CXCR2 deletion is time dependent and irreversible. Peripheral blood cells collected from *Cxcr2*$^{fl/fl}$*::Mx-Cre*$^{+}$ mice before injection, at 2 wks, 3 wks, 4 wks, and 18 wks after poly(I:C) injection, were stained with Ly6GFITC and CXCR2PE antibodies and were analyzed by flow cytometry. The percentage indicated in the figures is CXCR2 positive neutrophils in the total peripheral blood cells. These data represent at least three independent experiments.

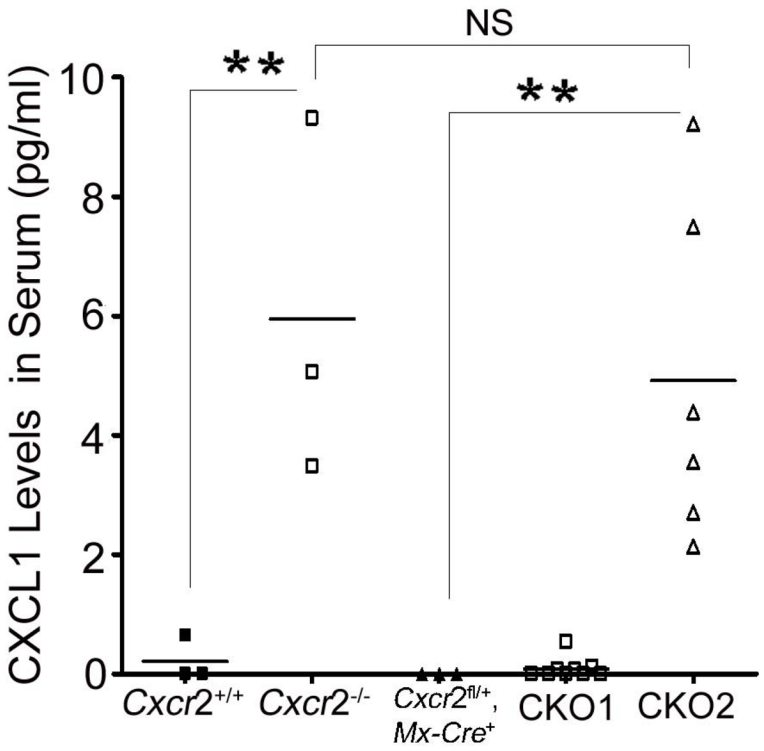

Figure 4. CXCR2-deficient neutrophils show defective ligand scavenging

ELISA assays for CXCL1 were performed on sera from *Cxcr2*$^{+/+}$, *Cxcr2*$^{-/-}$, *Cxcr2*$^{fl/fl}$ mice (data not shown), *Cxcr2*$^{fl/+}$*::Mx-Cre*$^{+}$ mice, CKO1 mice: CXCR2 deletion on neutrophils of *Cxcr2*-CKO mice is less than 90%, and CKO2 mice: CXCR2 deletion on neutrophils of *Cxcr2*-CKO mice is more than 90%. There is undetectable CXCL1 in the serum of *Cxcr2*$^{+/+}$ *Cxcr2*$^{fl/fl}$ mice (data not shown), *Cxcr2*$^{fl/+}$*::Mx-Cre*$^{+}$ mice and CKO1 mice. However, there is detectable CXCL1 in *Cxcr2*$^{-/-}$ mice and CKO2 mice. N is indicated by spots. Each spot represent one mouse on each group; **P<0.01, significant difference. NS: no significant difference. These data represent two independent experiments.

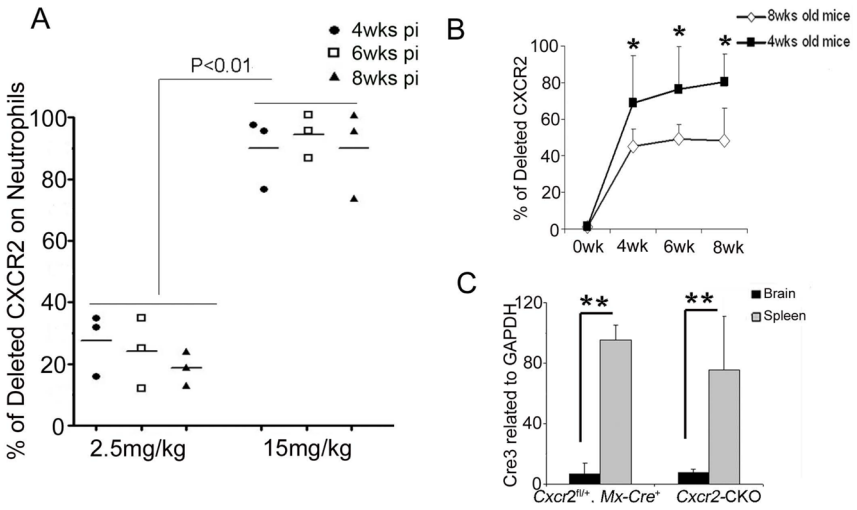

Figure 5. Dose-dependent recombination induced by poly(I:C) in periphery, not CNS, of *Cxcr2*-CKO mice

(A) 4 wk old *Cxcr2*$^{fl/fl}$*::Mx-Cre*$^{+}$ mice were given the indicated doses of poly(I:C) and CXCR2 deletion on neutrophils was examined by flow cytometry at 4 wks, 6 wks, and 8 wks post injection (pi). (B) 4 wks or 8 wks old mice were injected with 5 mg/kg of polyI:C. The deletion of CXCR2 was measured before injection, 4 wks, 6 wks and 8 wks after injection. N= 3 or 4 each group as indicated. The data represent two independent experiments. *P<0.05 (C) *Cre* recombinase expression in the spleen and brain 4 wks after poly(I:C) injection. Total RNA of brain and spleen tissues was extracted from *Cxcr*2-CKO and *Cxcr2*$^{fl/+}$*::Mx-Cre*$^{+}$mice. Real time PCR for Cre was performed on cDNA synthesized from 1ug of RNA. N=3 each group. These data represent two independent experiments. **P<0.01;

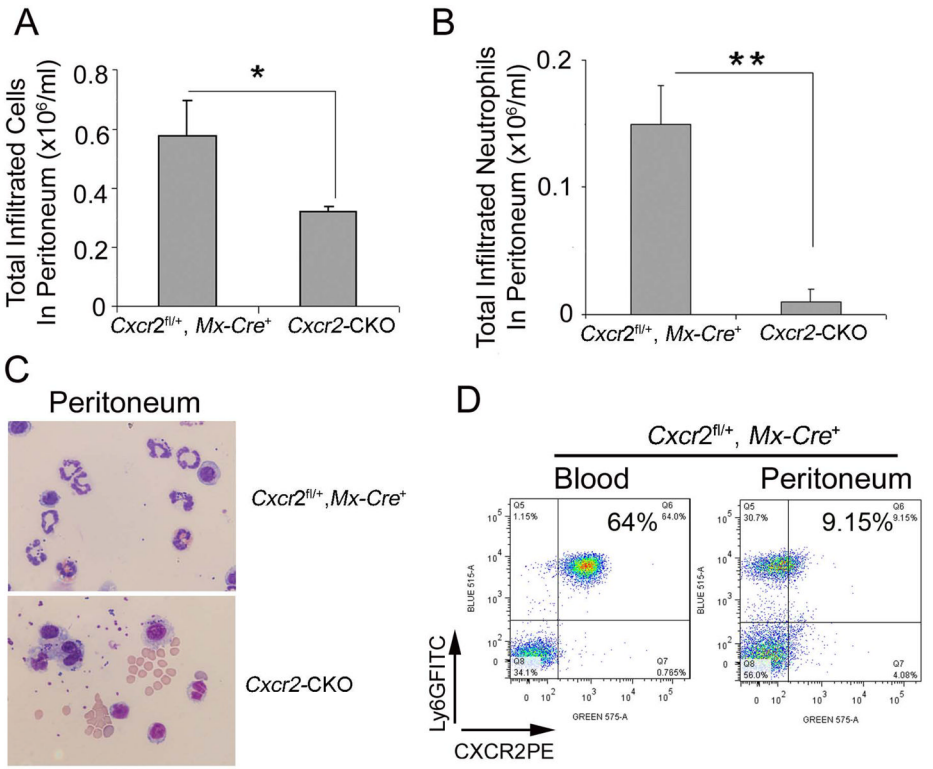

Figure 6. Decreased migration of CXCR2-deficient neutrophils in sterile peritonitis

*Cxcr*2-CKO and *Cxcr2*$^{fl/+}$*::Mx-Cre*$^{+}$ mice 4 wks after poly(I:C) injection were injected with 4% aged TG 2 hours before analysis. (A) Total cells were collected from the peritoneum and counted on a hemocytometer. (B) Total infiltrated neutrophils in peritoneum were calculated by total cells collected from the peritoneum times the percentage of neutrophils in total cells determined by the staining of peritoneal cells with Ly6G and CD45 antibodies (data not shown). (C) Wright-Giemsa staining of peritoneal cells collected by cytospin showed neutrophils with multiple lobulated nuclei in the peritoneal exudate of *Cxcr2*$^{fl/+}$*::Mx-Cre*$^{+}$mice (top) and mononuclear and kidney-shaped nuclei consistent with monocytes in the peritoneum of *Cxcr*2-CKO mice (bottom). (D) Peritoneal exudate cells and blood cells from *Cxcr2*$^{fl/+}$*::Mx-Cre*$^{+}$ mice were collected and stained with Ly6G and CXCR2 antibodies, then analyzed by flow cytometry. These data represent two independent experiments. Each experiment included 3 mice per group. **P<0.01; *P<0.05;